On the Fast Solar Wind Heating and Acceleration Processes: A Statistical Study Based on the UVCS Survey Data

Daniele Telloni [ORCID], Silvio Giordano [ORCID], and Ester Antonucci [ORCID]
National Institute for Astrophysics—Astrophysical Observatory of Torino Via Osservatorio 20, I-10025 Pino Torinese, Italy; daniele.telloni@inaf.it
Received 2019 July 16; revised 2019 July 30; accepted 2019 July 31; published 2019 August 20

Abstract

The UltraViolet Coronagraph Spectrometer (UVCS) on board the *SOlar and Heliospheric Observatory* has almost continuously observed, throughout the whole solar cycle 23, the UV solar corona. This work addresses the first-ever statistical analysis of the daily UVCS observations, performed in the O VI channel, of the northern polar coronal hole, between 1.5 and 3 $R_\odot$, during the period of low solar activity from 1996 April to 1997 December. The study is based on the investigation, at different heights, of the correlation between the variance of the O VI 1031.92 Å spectral line and the O VI 1031.92, 1037.61 Å doublet intensity ratio, which are proxies of the kinetic temperature of the O^{5+} ions and of the speed of the oxygen component of the fast solar wind, respectively. This analysis allows the clear identification of the sonic point in polar coronal holes at the distance of 1.9 $R_\odot$. The results show that heat addition below the sonic point does not lead to an increase of the outflow speed. As a matter of fact, the coronal plasma is heated more efficiently in the subsonic region, while its acceleration occurs more effectively in the region of supersonic flow. So, within the panorama of the *Parker Solar Probe* and *Solar Orbiter* missions, the statistical analysis of the historical UVCS data appears to be very promising in providing unique clues to some still unsolved problems, as the coronal heating, in the solar corona.

Unified Astronomy Thesaurus concepts: The Sun (1693); Solar corona (1483); Solar coronal heating (1989); Solar wind (1534)

1. Introduction

The first in situ interplanetary observations performed at the very beginning of the space era, in the early 1960s, definitely proved the Parker (1958) prediction of the existence of a supersonic solar wind, continuously flowing through the interplanetary space and transporting magnetized solar plasma to the Earth orbit and beyond, filling the entire heliosphere. The detailed empirical knowledge of the interplanetary medium derived from the first years of space exploration was summarized by Hundhausen (1972), where the solar wind fundamental properties were presented in a thorough manner. The space observations obtained by the Russian deep space probes *Luna 2*, *Luna 3*, and Venus 3, launched between 1959 and 1961, and the U.S. space probe *Explorer 10*, launched in 1961, confirmed the presence of a flux of positive ions in the interplanetary space. Soon after, the *Mariner 2* spacecraft, sent to Venus in late 1962, established the existence of a solar wind and showed that the variations in the solar wind properties were dominated by high-speed streams with outflow velocity up to about 800 km s^{-1} (Neugebauer & Snyder 1966, 1967).

Several authors in the early 1970s suggested that high-speed streams observed in the solar wind might originate from magnetically open regions in the corona rather than from higher-temperature regions. Munro & Withbroe (1972), in a study of *OSO*-4 EUV data obtained in 1967, suggested that coronal holes, defined as vast regions where the density and temperature are exceptionally low, are associated with diverging magnetic fields. An assessment of the energy flux escaping into space from a coronal hole region led Noci (1973) to the conclusion that coronal holes are the likely sources of the high-speed streams observed in the solar wind. Krieger et al. (1973) found a striking agreement between the Carrington longitude of the solar source of a recurrent high-speed stream and the position of a hole observed in 1970, in

X-rays, during a rocket flight. The Skylab high-resolution X-ray images (Vaiana et al. 1974) did confirm the scenario emerging from these earlier observations: that is, the near-equatorial coronal holes, observed as weak emission regions in EUV, X-rays, and radio, and characterized by open, diverging, unipolar magnetic fields, are the sources of the high-speed wind streams detected in the ecliptic plane (e.g., Nolte et al. 1976). Two decades elapsed before the properties and evolution of the solar wind were measured out of the ecliptic. During its 18 years of exploration (1990–2008) of the three-dimensional solar wind, the *Ulysses* probe twice crossed the high-latitude (up to 80° latitude) northern and southern regions of the heliosphere over the solar poles during minimum solar activity. The *Ulysses* observations established that during solar minimum (cycles 22 and 23) the fast solar wind was filling most of the heliosphere, while the slower variable solar wind was confined to lower latitudes (McComas et al. 2008).

The advent of the ultraviolet spectroscopy of the extended corona, performed with the UltraViolet Coronagraph Spectrometer (UVCS; Kohl et al. 1995) on board the *SOlar and Heliospheric Observatory* (*SOHO*; Domingo et al. 1995) in the time interval 1995–2012, allowed at last the identification of the coronal regions where the high-speed wind undergoes the acceleration process and reaches approximately its asymptotic speed. The expansion velocity of the coronal plasma in the polar regions was measured from 1.5 to 5 $R_\odot$, by adopting the Doppler dimming technique applied to the resonantly scattered UV lines emitted by neutral hydrogen and ions such as O^{5+}, as proposed by Noci et al. (1987). The expansion velocity of the hydrogen component of the solar wind, which is representative of the proton component out to approximately 3 $R_\odot$, increases up to 2–300 km s^{-1} at 3 $R_\odot$, while the oxygen component increases up to a upper level of about 800 km s^{-1} at about 5 $R_\odot$ (Kohl et al. 1997, 1998;

Dodero et al. 1998; Cranmer et al. 1999; Antonucci et al. 2000; Giordano et al. 2000; Telloni et al. 2007a).

Since the first UVCS spectroscopic observations of polar coronal holes, the unexpected extremely broad profiles of the O VI 1031.92 and 1037.61 Å lines and the highly anisotropic velocity distribution across the magnetic field of the oxygen ions (see reviews by Antonucci 2006; Kohl et al. 2006; Antonucci et al. 2012) have been interpreted as the most remarkable signatures of the processes acting in the outer corona to heat the coronal plasma and to accelerate the solar wind. The observed preferential energy deposition perpendicular to the field lines points to the ion cyclotron dissipation of Alfvén waves as a likely mechanism for the heating of the oxygen wind component (Kohl et al. 1998; Cranmer et al. 1999). The coronal region where these mechanisms are more efficient has been identified between 2 and 3.7 $R_\odot$ (Telloni et al. 2007b).

All the above papers report case studies: the corresponding results may therefore suffer from the particular conditions of the coronal plasma properties at the time the UVCS instrument observed the corona. In order to account for the temporal variability of the coronal dynamics and thus provide more reliable results, a statistical study should be accomplished. Moreover, patterns and correlations are clear and visible only when large samples of data are used for the analysis. Therefore, some results such as the efficiency of the processes underlying the coronal plasma heating and the solar wind acceleration, as well as the identification of the sonic point and of the region where energy is preferentially deposited to lift the high-speed wind in the corona, can be provided only by means of a statistical investigation of the UVCS data. In this Letter, the study of the high-speed solar wind is hence performed over the entire set of UVCS data available during the solar cycle (cycle 23) for a polar region 10° wide centered on the polar axis in the northern hemisphere with a latitude extension from 1.5 to an upper level of 3 $R_\odot$. The analysis is limited to the oxygen component of the solar wind, which allows us to derive the coronal expansion speed based on the O VI 1031.92, 1037.61 Å line ratio.

2. UVCS Observations

The spectroscopic measurements of the solar corona provided by UVCS on board *SOHO*, operating at the Lagrangian point L1, have been acquired almost continuously from 1996 to 2012. The UVCS instrument has two UV spectrometric channels, optimized for the observation of the H I Lyα spectral line at 1215.7 Å and of the O VI doublet (1031.92 and 1037.61 Å). The UVCS slit, delimiting a field of view 40′ long and up to 84″ wide, can be positioned at any heliocentric distance within 1.2 to 10 $R_\odot$, and at any roll angle from 0° to 360° from the northern pole counterclockwise. This investigation is focused on the minimum activity period of solar cycle 23 (from 1996 April to 1997 December), when the solar corona was characterized by stable, long-lived polar coronal holes and a near-equatorial streamer belt configuration. In order to study the sources of high-speed streams during the solar minimum, a narrow region 20° wide is selected around the northern polar axis, where the O VI doublet is roughly daily observed at different heights from 1.5 to 3 $R_\odot$. The daily UVCS synoptic observation program thus provides a statistically significant, almost uninterrupted (the time coverage is of about 89%, data gaps being mostly due to telemetry losses) data set of the

intensity and width of the O VI doublet spectral lines, in the core of polar holes, where the coronal plasma is heated and accelerated to form the fast solar wind. The heliocentric distance of the UVCS instantaneous field of view for each observation performed in the O VI channel with the same instrumental setup (that is, a slit width of 300 μm and a spectral resolution of 0.6 Å) during the entire period selected for the analysis is shown as a function of the observation time in Figure 1(a). The corresponding intensities of the O VI doublet lines at 1031.92 Å (in black) and at 1037.61 Å (in red) are shown in Figure 1(b).

The O VI spectroscopic measurements allow the estimation of quantities representative, to a first approximation, of the radial outflow speed and the kinetic temperature of the oxygen ions.

The O VI 1037.61 and 1031.92 Å lines are formed during the atomic transition from ground level 1 to levels 2 and 3, respectively, and can be thus denoted as I_{12} and I_{13}, respectively. Their ratio $\rho = I_{12}/I_{13}$ can be expressed as

$$\rho = \frac{I_{12}}{I_{13}} \sim \frac{C_{12}N_1 + 4\pi j_{12}/h\nu_{12}}{C_{13}N_1 + 4\pi j_{13}/h\nu_{13}}, \qquad (1)$$

where the approximation comes from considering the emission on the plane of the sky as the most significant contribution to the coronal profile. In Equation (1), C_{jk} is the collisional excitation rate from level j and level k, ν_{jk} is the frequency of the jk transition, j_{jk} is the emissivity for the resonant scattered component in the transition jk, and N_1 is the number density of scattering ions in the ground level.

The ratio of the O VI doublet intensities is thus a function of the electron density n_e and temperature T_e, of the O^{5+} velocity distribution (and, in turn, of the oxygen temperature perpendicular, $T_\perp$, and parallel, $T_\parallel$, to the magnetic field), and of the speed of the outflowing coronal plasma V, i.e., $\rho = \rho(n_e, T_e, T_\perp, T_\parallel, V)$. However, since all these quantities appear in both the factors of Equation (1), they slightly contribute to ρ, with an exception made for the outflow speed V. Indeed, because of the pumping on the O VI 1037.61 Å by the nearby C II lines at 1036.34 Å and 1037.02 Å, the O VI doublet lines are differently affected by the Doppler dimming, and therefore their intensity ratio $\rho = I_{1037.61}/I_{1031.92}$ is used as a powerful diagnostic tool to derive the speed of the oxygen component of the solar wind along the magnetic field lines (Noci et al. 1987; Dodero et al. 1998). It turns out that ρ is a proxy to study the dynamical properties of the coronal regions where the solar wind is accelerated. This quantity is shown for the UVCS measurements during the minimum phase of solar cycle 23 in Figure 1(c).

The kinetic temperature T_k of the O^{5+} ions is derived from the width σ of the more intense O VI 1031.92 Å spectral line, as $T_k = m(\sigma c/\lambda_0)^2/k_B$, where m is the oxygen mass, c is the speed of light, $\lambda_0 = 1031.92$ Å is the wavelength of the spectral line, and k_B is the Boltzmann constant. The broadening of the O VI line is due to unresolved motions along the line of sight, including the effects of both thermal and nonthermal (due, for instance, to turbulence or Alfvén waves propagating through the corona; Hollweg 1978) motions, perpendicular to the magnetic field that at the poles is predominantly radial. The variance, namely, the second-order moment, of the spectroscopic line profile, properly corrected for instrumental effects to primarily be a measure of ion velocity distribution, is thus proportional to T_k and is indeed used in the analysis as a proxy
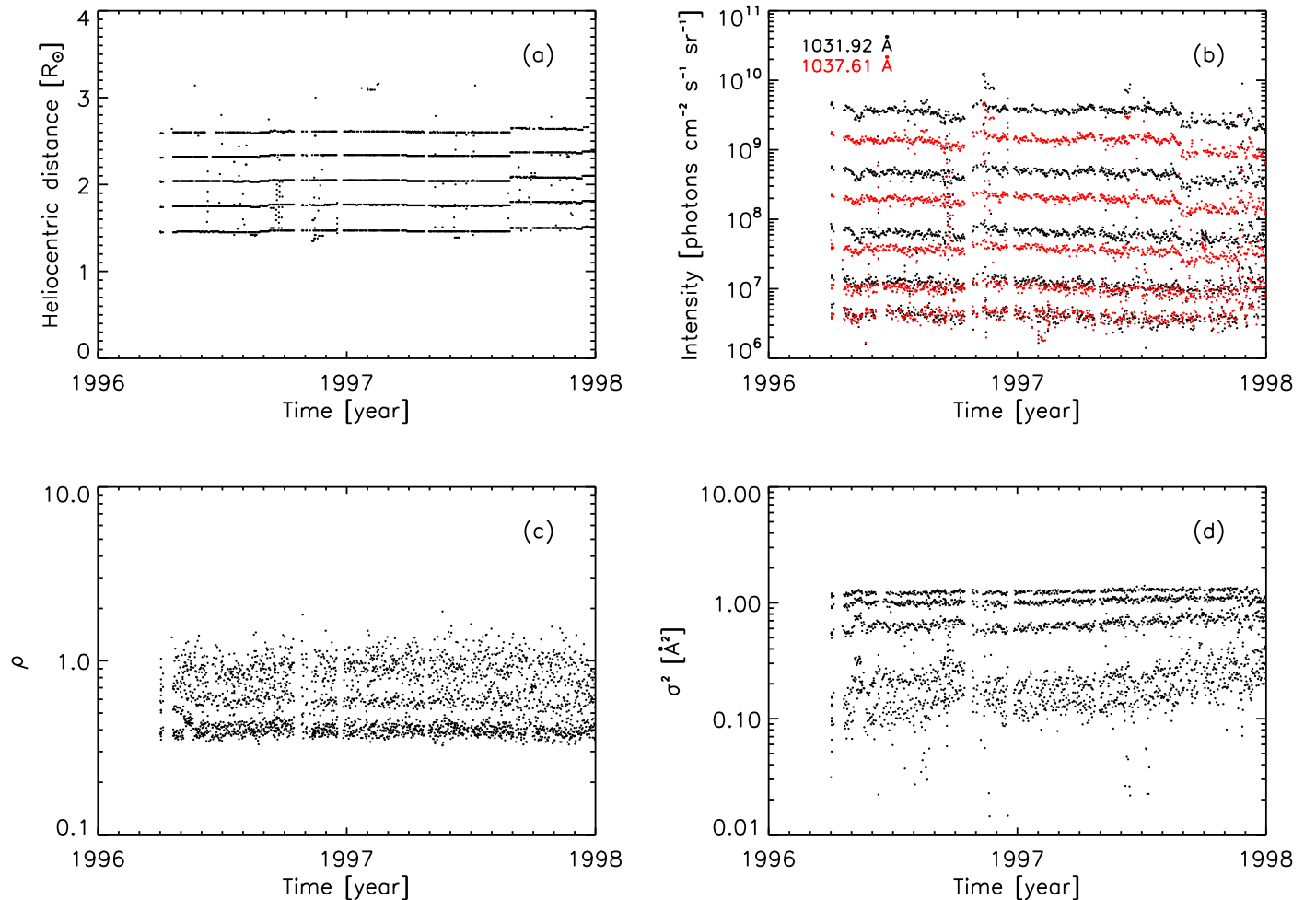
Figure 1. O VI channel parameters referring to the period from 1996 April to 1997 December during the daily UVCS synoptic observation program: heliocentric distance of the UVCS instantaneous field of view (a), intensity of the 1031.92 Å (black) and 1037.61 Å (red) spectral lines (b), doublet intensity ratio ρ (c), and variance of the 1031.92 Å line, corrected for instrumental effects, σ^2 (d).

of the oxygen kinetic temperature. This is shown, for the UVCS observations performed during the synoptic campaign, as a function of time, in Figure 1(c). It is worth noting that σ^2 provides an estimate of the oxygen temperature perpendicular to the magnetic field $T_\perp$, which exceeds the parallel temperature $T_\parallel$ beyond 1.8–2.0 $R_\odot$, where the O^{5+} velocity distribution has been proved to be anisotropic (e.g., Antonucci et al. 2000; Telloni et al. 2007b).

3. Analysis Results

The statistical distribution of the radial outflow speed (i.e., ρ) and the kinetic temperature (i.e., σ^2) of the oxygen component of the solar wind is shown in Figure 2(a), during the phase of minimum activity of solar cycle 23, as a function of the heliocentric distance (different colors refer to different heights above the solar limb). It is immediately evident as the two quantities are closely clustered in the $\rho - \sigma^2$ phase space, regardless of the particular distance from Sun center. If their correlation can be thought of as a proxy of the efficiency ϵ of the coronal heating and solar wind acceleration processes, the $\rho - \sigma^2$ clustering clearly indicates that the energy deposition across the magnetic field and its redistribution along the field lines occur as extremely steady-state mechanisms in the outer

corona, with very small perturbations throughout the solar minimum.

However, the efficiency ϵ varies moving outward within the extended corona. This quantity can be indeed inferred as the Spearman's rank correlation factor r of the two sample populations ρ and σ^2, as a function of the heliocentric distance. As shown in Figure 2(b), r increases with the height, though not diverging, rather converging, toward a certain limiting value, as suggested by the logarithmic fit (red curve). It turns out that the efficiency of the mechanism redistributing the energy (deposited perpendicularly to the magnetic field likely by ion cyclotron resonant Alfvén waves) radially to accelerate the high-speed wind increases with the altitude, until reaching a maximum near-balanced growth for a heliocentric distance slightly larger than 3 $R_\odot$.

The UVCS data statistical study also allows a robust identification of the sonic point r_c in the polar coronal holes. The sonic speed c_s is derived from the thermodynamic temperature of the solar coronal plasma (that is, the electron temperature) T, as $c_s = \sqrt{2k_B T/m_p}$, where k_B is the Boltzmann constant and m_p is the proton mass. The coronal hole electron temperature deduced from the measurements of the *SOHO* instruments is $\lesssim 8 \times 10^5$ K (Noci 2003). As a result, for a typical coronal hole observed during the solar minimum, the sonic speed c_s is about 100 km s^{-1}, which roughly corresponds
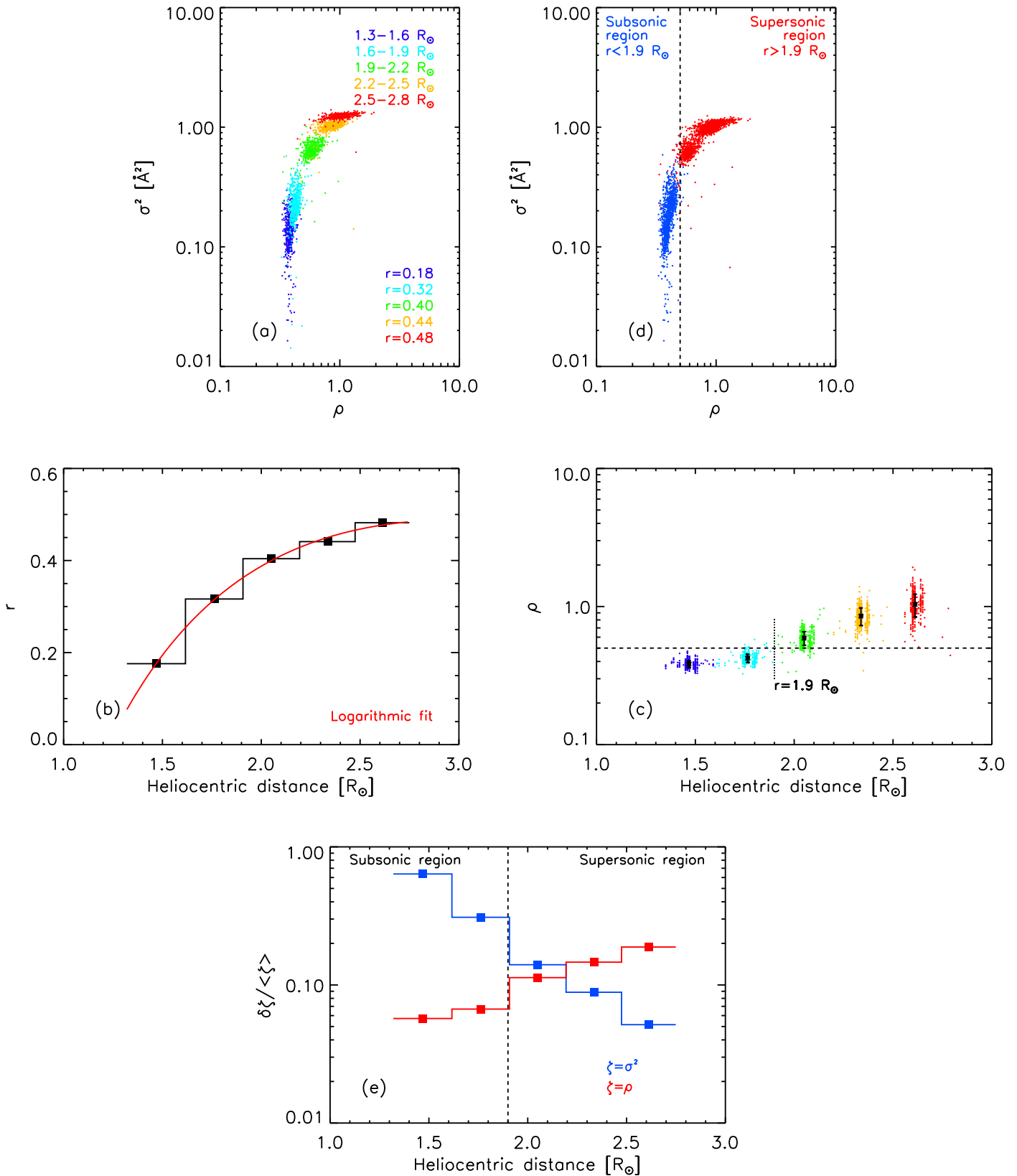
Figure 2. (a) $\rho - \sigma^2$ scatter plot for UVCS O VI observations performed between 1.3 and 2.8 $R_\odot$ (different colors refer to different distances as reported in the legend); the corresponding values of the Spearman's rank correlation factor r are also shown. (b) Radial profile of the correlation factor r fitted with a logarithmic function (red curve). (c) Intensity ratio ρ as a function of the UVCS observation distance (colors are the same as used for panel (a)); the corresponding mean values and error bars (inferred from the standard deviation) are also displayed; $\rho = 0.5$ is marked by the dashed line; the sonic point $r_c \simeq 1.9\ R_\odot$ is indicated by the dotted line. (d) $\rho - \sigma^2$ scatter plot in the subsonic (blue) and supersonic (red) regions, separated by the $\rho = 0.5$ dashed line. (e) Radial profile of the amplitude of the ρ (red) and σ^2 (blue) fluctuations, normalized to the corresponding average values; the dashed line marks the sonic point r_c, separating regions of subsonic and supersonic flow.

to an intensity ratio ρ of 0.5. Indeed, as clearly shown by Noci et al. (1987) $\rho \simeq 0.5$ for an outflow speed of about 100 km s^{-1}, independently of the value of other physical parameters. It turns out that $\rho \gtrless 0.5$ identifies the supersonic (subsonic) coronal regions where the plasma is moving at speeds higher (lower) than 100 km s^{-1}.

Figure 2(c) displays the ratio ρ inferred from the O VI doublet intensity measurements acquired by UVCS during the daily synoptic program from 1996 April to 1997 December, as a function of the UVCS observation distance. For heliocentric distances smaller (larger) than 1.9 $R_\odot$, ρ assumes values below (above) 0.5 (dashed horizontal line). Therefore, the sonic point in polar coronal holes during the minimum of the solar activity can be statistically located at the distance $r_c \simeq 1.9\ R_\odot$.

The study of how ρ and σ^2 are distributed in the subsonic and supersonic coronal regions provides interesting information about the heat addition in the fast solar wind, considering that ρ is predominantly a proxy of the outflow speed, even if it depends, but to a lesser degree, also on other physical quantities, as discussed in Section 2. In Figure 2(d), blue (red) dots refer to ρ and σ^2 values estimated at heliocentric distances below (above) the sonic point $r_c \simeq 1.9\ R_\odot$. Outflow speed and kinetic temperature observations are weakly correlated in the subsonic region, while they are strongly correlated at supersonic heights. This clearly indicates that heating of the coronal plasma in the subsonic region has little effect on the outflow speed. On the other hand, when the corona is heated above the sonic point the solar wind speed is effectively increased. This observational result represents a statistical validation of the theoretical predictions by Leer & Holzer (1980) for thermally driven winds that heating below the sonic point increases density, while heating above the sonic point increases velocity.

A further interesting result can be outlined from Figure 2(a). It is indeed clearly evident that the variability of the ρ and σ^2 values change with the height above the solar limb. The fluctuation amplitude $\delta\zeta$ of a generic quantity ζ, normalized to its average value $\langle\zeta\rangle$ and expressed as $\delta\zeta/\langle\zeta\rangle = \sqrt{\langle\zeta^2\rangle - \langle\zeta\rangle^2}/\langle\zeta\rangle$, can be used to assess the variability of ζ. Figure 2(e) shows this estimation for ρ (red) and σ^2 (blue), as a function of the heliocentric distance. While the variability of the values assumed by the oxygen kinetic temperature exponentially decreases with increasing the altitude, the variability of ρ (which is primarily, though not solely, associated with the variability of the speed of the oxygen component of the solar wind) grows, particularly above r_c in the supersonic region. This observational evidence can be quite easily interpreted, having in mind that the amplitude of the fluctuations of any solar wind parameter is related to the energy associated with the mechanism underlying its modulation. In this scenario, the damping of the amplitude of the temperature fluctuations with the height suggests that less and less energy is available to heat the coronal plasma moving outward within the extended corona, according to the observation that the oxygen kinetic temperature flattens at large heliocentric distances (Telloni et al. 2007a). Conversely, the mechanism that, in response to the heating across the magnetic field, redistributes the energy along the field lines, accelerating the O^{5+} ions to outflow velocities of $\sim$800 km s^{-1} at about 5 $R_\odot$ (Telloni et al. 2007a), is expected to become more effective with increasing heliocentric distance. The energy transfer and consequent acceleration mechanism would make more and more energy available in the radial direction, thus leading to an enhancement of the outflow speed fluctuations,

particularly in the region of the supersonic flow, where the acceleration processes are fully effective.

4. Concluding Remarks

The main benefit of statistical investigations over case studies resides in the capability of unambiguously identifying the coronal regions where the physical processes underlying the coronal heating and solar wind acceleration are most effective and in quantifying some important solar wind parameters. The statistical analysis of daily UVCS observations performed in the O VI channel at different heights above the northern polar coronal hole, during the low-activity phase of solar cycle 23, has led to a number of crucial results. (i) The mechanisms at the base of the heating and acceleration of the fast solar wind plasma have been proven to be extremely steady. (ii) It has been shown that the efficiency of the redistribution of the energy deposited across the magnetic field, along it, to lift the high-speed wind, increases with the heliocentric distance, until stabilizing at large altitudes. (iii) The sonic point r_c in polar coronal holes has been statistically set at 1.9 $R_\odot$, and it has been definitively validated that heat addition leads to solar wind acceleration only when the energy is deposited in the region of supersonic flow. (iv) During the expansion of the coronal plasma, the variability of the outflow speed increases while that of the kinetic temperature lessens: this is a clear indication that energy is progressively transferred from the transverse to the radial direction, enhancing the variability parallel to the magnetic field at the expense of the perpendicular one.

It would be very interesting also to extend this analysis to periods of maximum activity during the solar cycle, in order to study how and where the above processes are modulated during the solar cycle phases. However, this is devoted to a future work.

ORCID iDs

Daniele Telloni ⬤ https://orcid.org/0000-0002-6710-8142
Silvio Giordano ⬤ https://orcid.org/0000-0002-3468-8566
Ester Antonucci ⬤ https://orcid.org/0000-0003-4155-6542

References

Antonucci, E. 2006, SSRv, 124, 35
Antonucci, E., Abbo, L., & Telloni, D. 2012, SSRv, 172, 5
Antonucci, E., Dodero, M. A., & Giordano, S. 2000, SoPh, 197, 115
Cranmer, S. R., Kohl, J. L., Noci, G., et al. 1999, ApJ, 511, 481
Dodero, M. A., Antonucci, E., Giordano, S., & Martin, R. 1998, SoPh, 183, 77
Domingo, V., Fleck, B., & Poland, A. I. 1995, SoPh, 162, 1
Giordano, S., Antonucci, E., & Dodero, M. 2000, AdSpR, 25, 1927
Hollweg, J. V. 1978, RvGSP, 16, 689
Hundhausen, A. J. 1972, Coronal Expansion and Solar Wind (New York: Springer), 101
Kohl, J. L., Esser, R., Gardner, L. D., et al. 1995, SoPh, 162, 313
Kohl, J. L., Noci, G., Antonucci, E., et al. 1997, SoPh, 175, 613
Kohl, J. L., Noci, G., Antonucci, E., et al. 1998, ApJL, 501, L127

Kohl, J. L., Noci, G., Cranmer, S. R., & Raymond, J. C. 2006, A&ARv, 13, 31
Krieger, A. S., Timothy, A. F., & Roelof, E. C. 1973, SoPh, 29, 505
Leer, E., & Holzer, T. E. 1980, JGR, 85, 4681
McComas, D. J., Ebert, R. W., Elliott, H. A., et al. 2008, GeoRL, 35, L18103
Munro, R. H., & Withbroe, G. L. 1972, ApJ, 176, 511
Neugebauer, M., & Snyder, C. W. 1966, JGR, 71, 4469
Neugebauer, M., & Snyder, C. W. 1967, JGR, 72, 1823
Noci, G. 1973, SoPh, 28, 403
Noci, G. 2003, MmSAI, 74, 704
Noci, G., Kohl, J. L., & Withbroe, G. L. 1987, ApJ, 315, 706
Nolte, J. T., Krieger, A. S., Timothy, A. F., et al. 1976, SoPh, 46, 303
Parker, E. N. 1958, ApJ, 128, 664
Telloni, D., Antonucci, E., & Dodero, M. A. 2007a, A&A, 472, 299
Telloni, D., Antonucci, E., & Dodero, M. A. 2007b, A&A, 476, 1341
Vaiana, G. S., Krieger, A. S., Petrasso, R., Silk, J. K., & Timothy, A. F. 1974, Proc. SPIE, 44, 185